Comparison and Evaluation of CNN Architectures for Classification of Covid-19 and Pneumonia

Adwait Mahadar
School of Computer Science and Engineering
Dr. Vishwanath Karad MIT World Peace University, Pune
Pune, India
adwaitmahadar@gmail.com

Priyen Mangukiya
School of Computer Science and Engineering
Dr. Vishwanath Karad MIT World Peace University, Pune
Pune, India
pmangukiya312@gmail.com

Trupti Baraskar
School of Computer Science and Engineering
Dr. Vishwanath Karad MIT World Peace University, Pune
Pune, India
trupti.baraskar@mitwpu.edu.in

2021 Sixth International Conference on Image Information Processing (ICIIP) | 978-1-6654-3361-7/21/$31.00 ©2021 IEEE | DOI: 10.1109/ICIIP53038.2021.9702676

Abstract*— At present, India has the largest population of below 14 years children in the Asia Pacific. With the increasing birth rate, critical Pneumonia cases have been referred to Neonatal Hospital for treatment. As the number of adults in India who have tested positive for COVID-19 has grown, so has the number of children who have contracted it. However, we haven't noticed a dramatic increase in the number of children infected with COVID-19 across the country. It's important to note that, unlike the previous wave, the second wave is more likely to infect whole homes. We must be vigilant and adhere to COVID-19's recommended practices. The current study says that the mortality rate of Pneumonia and Covid-19 infection in rural areas is high. Radiology plays a vital role to diagnose Pneumonia by the examination of X-Ray images. Over the years CNN Architectures have evolved and now produce appreciable accuracy (over 85%) for classification tasks. This has promoted the use of CNN Architectures in the field of medicine, especially for classification tasks such as disease detection from x-rays. This implementation evaluates the performance of four popular CNN Architectures viz. VGG16, ResNet50V2, InceptionV3 and MobileNetV2. The implementation will classify x-ray images into normal, covid, and pneumonia and then compare the performance of the aforementioned models over the accuracy, Area under the curve (AUC), precision, recall metrics.

Keywords*—Convolution Neural Network, X-ray Images, Pneumonia, Covid-19, Classification, Medical Classification.

I. Introduction

Pneumonia is a contagion that affects the human lungs very easily. The respiratory system is infected with viral illnesses such as strep throat, tonsils, and influenza that can develop into Pneumonia, which can create a serious infection in the human lungs. There are different types of Pneumonia i.e., Waking, Viral, Bacterial, Chemical. Health professionals use few terms like Hospital-acquired pneumonia and Community-acquired pneumonia [1]. This infection can often be diagnosed with a thorough history and physical examination. For diagnosing pneumonia, doctors review the medical history and perform a clinical investigation such as a chest X-ray. Using those reports and proofs, doctors can determine what type of pneumonia has affected the patient. Pneumonia treatment might include antibiotics, fungal or viral medicines. In case of severe pneumonia, the patient might need to get hospitalized for oxygen therapy, and antibiotics are given through an intravenous line. Chest X-Ray is an efficient imaging technique which allow radiologists to diagnose a patient's lungs, heart, and blood vessels to determine if a patient is suffering from pneumonia. Fig. 1 gives the information related to the evaluation of Chest X-rays by Radiologists. Fig. 2 gives the list of Pneumonia tests that may be used by doctors to evaluate Pneumonia [2]. The study, detection, and classification of COVID-19, Pneumonia-infected, and normal Chest X-ray images is a very tedious task for radiologists. To overcome this task and for accurate prediction of different infectious diseases Convolution Neural Network Architectures play a major role [3][4].

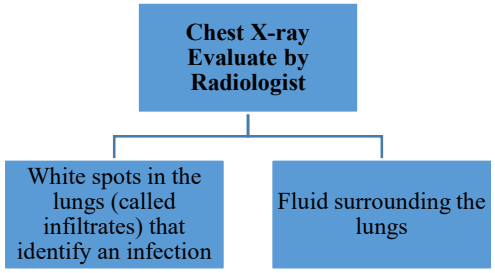

Fig. 1 Evaluation Methods used by Radiologist

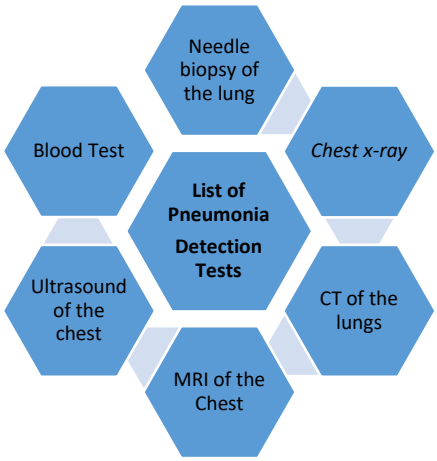

Fig.2 List of Pneumonia Detection Tests

II. Related Work

In the past twenty years, Deep Learning techniques provide a number of architectures and algorithms. These Deep Learning Architectures are divided into supervised and unsupervised learning. Supervised learning introduces two popular architectures; Convolution Neural Network (CNNs) and Recurrent Neural Network (RNNs). The CNNs are particularly useful in Computer Vision, Video Analysis, Image Processing Applications [5-7]. Normally the CNNs are designed using several deep layers of processing that are useful for primary feature extraction and further classification

[8]. The CNNs mainly categorize into several classes such as Depth Based, Spatial Exploitation, Multi Path Based, Width Based Multi – Connection [9-10]. The VGG16 comes into Spatial Exploration Based CNN. This architecture gives good result for x-ray classification and Pneumonia detection/ prediction [11-12]. This study paper [13] has designed a simple VGG Based CNN module which obtained 88.07% accuracy 91.41% precision rate for detection of Pneumonia. This study paper [14-15] has selected Resnet-50 which was trained using transfer learning method which gives 90.76% accuracy. The MobileNet and InceptionV3 models come into Depth-Based CNNs. This paper under study [16] employs the InceptionV3 model and achieves an accuracy of 94.42%. The study paper [17] demonstrates the use of MobileNet Architecture for pneumonia classification and obtains an accuracy of 92.79%.

III. PROPOSED MODEL

The chest x-ray images are divided into train, test, and validation sets. Further, the model is fed data from chest x-ray scans. Resizing is done for those images, as an appropriate size is required by the different Neural Network Architecture. Freezing the base layers of selected neural network models and removal of their top layers is performed during transfer learning. Then new layers are created on top of the base model in order to perform the covid, pneumonia classification task. Once transfer learning is done, all the resized images are then given as input to the selected CNN Architectures (wiz. VGG-16, MobileNetV2, InceptionV3, ResNet50V2). The entire model (including the base and top model) is set up for training. After training, the performance evaluation of developed CNN architecture will be tested for classification of infected X-ray, COVID-19, and normal X-ray Images. Then the CNN models are tuned in order to extract the best accuracy. Once a good accuracy is achieved, the models are compared with other CNN Architectures. The comparison is done on the accuracy, Area Under the Curve (AUC), precision, recall metrics. Below fig. 3 shows the proposed Deep Learning Model.

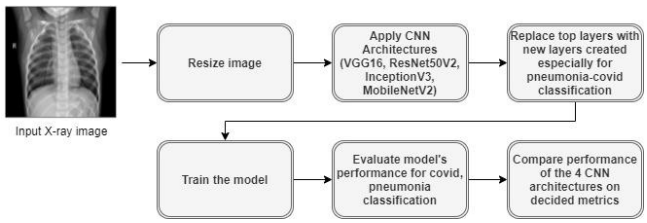

Fig.3 Schematic representation of the suggested Deep Learning Model.

IV. TRANSFER LEARNING AND CNN ARCHITECTURES

Training deep CNN architectures such as VGG, ResNet, Inception and MobileNet from scratch demands a huge amount of data as these architectures involve training parameters numbering in the millions.

A. Transfer learning

Transfer Learning also known as inductive learning is a supervised learning procedure used in deep learning, that reuses parts of a previously trained model developed for another task, is used as a starting point on a new network tasked for a different but similar problem. As part of deep learning systems, the approach of transfer learning is widely used in which as a preliminary step, a pre-trained model is used on natural language processing and computer vision tasks. Below Fig. 4 shows Transfer Learning Process.

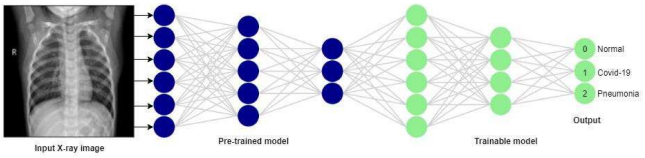

Fig.4 Transfer Learning Process

When an image is processed in a deep convolutional neural network, its essential features are detected in the early layers, such as edges or color while on the other hand, deeper layers are concerned with recognizing high-level features. In our study, we have used VGG, ResNet, Inception and MobileNet architectures pre-trained on ImageNet weights, as our based models on top of which few layers were added for the classification of x-rays into normal, covid, or pneumonia.

B. Pre-trained CNN architectures

In this study, we have implemented four different pre-trained models, VGG16, ResNet50V2, InceptionV3, and MobileNetV2, pre-trained on ImageNet dataset and applied them to the chest x-ray dataset. These CNN architectures were chosen as they belong to three different classes of Deep CNNs. VGG16 is a Spatial Exploitation based CNN while, InceptionV3 and MobileNetV2 are Depth based CNN's whereas, ResNet50V2 is a multi-Path based CNN. Fig. 5 below, shows the Hierarchical representation of Deep CNNs.

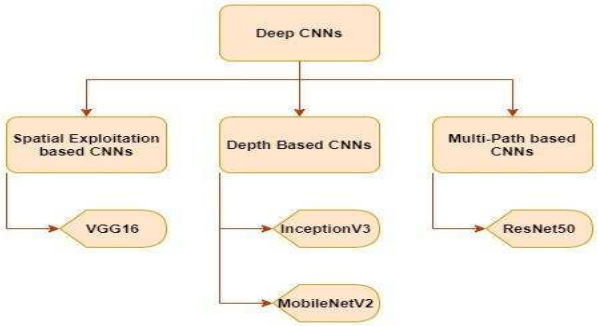

Fig.5 The Hierarchy of Deep CNNs.

1. VGG16

VGG16 when trained on ImageNet, a collection of 14 million-plus images distributed among thousand classes, achieves an accuracy of 92.7 percent. There are numerous 3x3 kernel size filters in the first and second convolutional layers, which helps it beat AlexNet.

VGG-16 has 16 layers with Kernel size is 3x3 for VGG-16, and pool size is 2x2 for all layers. On top of it, there is a softmax classifier. The algorithm is based on convolutional layers that increase depth and max pooling. Fig. 6 below shows the use of VGG16 for covid pneumonia detection.

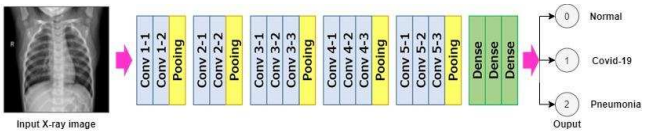

Fig. 6 VGG16 CNN Architecture

2. ResNet50V2

In order to speed up the training of networks that are considerably deeper than those previously used, Microsoft researchers created a residual learning framework. ResNet

uses a method known as "residual mapping" to solve this problem. ResNets are quite simple to understand when compared to traditional neural network topologies. When you add the shortcut connection, the network becomes its residual counterpart. This option does not add any new parameters to the equation. Depending on the ResNet version, each block is either two layers deep like ResNet 18 or 34, or three levels. ResNet 50, 101, or 152 are examples of such networks. Pre-activation of weight layers rather than post-activation is the focus of ResNet50 version 2. Fig. 7 below shows the use of ResNet50V2 for covid pneumonia detection.

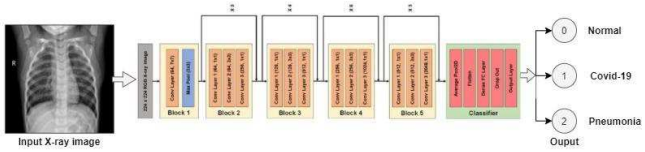

Fig. 7 ResNet50V2 CNN Architecture

3. InceptionV3

The Inception-v3 architecture is a convolutional neural network architecture from the Inception family that is widely used as an image recognition model.

It is commonly accomplished by pooling processes. The concepts of factorized convolutions, asymmetric convolutions, auxiliary classifier, and grid size-reduction are integrated into the final architecture. Fig.8 below shows the use of IncptionV3 for covid pneumonia detection.

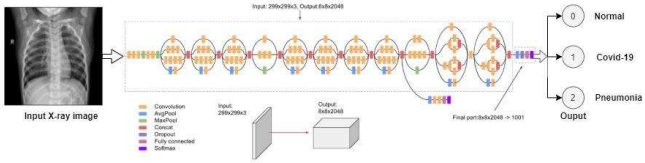

Fig.8 InceptionV3 CNN Architecture

4. MobileNetV2

MobileNet is a streamlined architecture that provides an efficient model for mobile and embedded vision applications. In MobileNetV2 the residual connections between the bottleneck layers are constructed using an inverted residual structure. The intermediary expansion layer filters features as a source of non-linearity using lightweight depth wise convolutions. Fig. 9 below shows the use of MobileNetV2 for covid pneumonia detection.

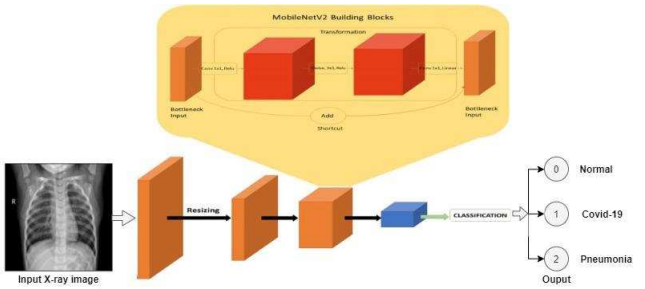

Fig. 9 Mobile Net V2 CNN Architecture

V. DATA INFORMATION

The dataset is sourced from Kaggle. It contains an eclectic sample of X-ray pictures of COVID19 due to the dearth of a single large dataset. First of all, 1401 COVID19 samples were collected using GitHub archive [18] the Radiopaedia, Italian Society of Radiology (SIRM), Figshare data repository websites[19]. Moreover, rather than deliberately applying data augmentation methods, 912 already augmented x-ray images were collected from Mendeley [20]. Lastly, a total of 2313 samples of pneumonia and normal x-ray images were added from Kaggle [21].

A. Data Set

Separated into three folders (normal, COVID19, pneumonia infected) the dataset includes chest X-ray images. In total 6939 X-ray samples were used and 2313 instances were used for each occurrence.

This dataset is then separated into 3 main folders (train, test, validation), and inside each folder additional 3 folders were created (normal, covid, pneumonia). The train folder contains a total of 4857 images wherein 1619 normal, 1619 covid, and 1619 pneumonia images are present. The test folder contains a total of 1388 images wherein 463 normal, 462 covid and 463 pneumonia images are present. The validation folder contains a total of 694 images wherein 231 normal, 232 covid and 231 pneumonia images are present.

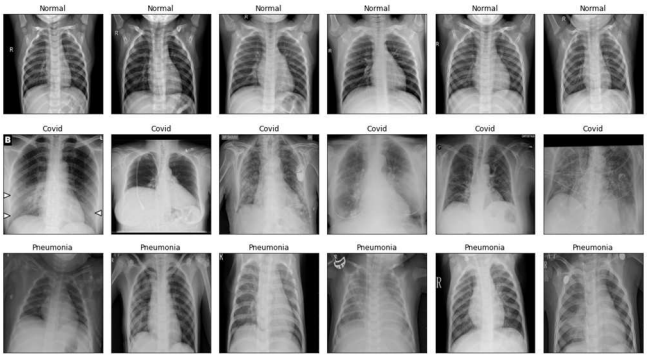

Fig. 10 Above Images shows the normal chest X-ray (top panel) illustrates clear lungs without any areas of abnormal opacification in the image. Whereas Covid infected X-ray (middle panel) and Pneumonia infected X-ray (bottom panel) typically exhibit certain opaqueness as demonstrated

B. Analysis of X-ray images:

To analyze our data we applied various filters and edge detectors to check whether an unskilled human eye can tell the difference between a normal and pneumonia infected x-ray.

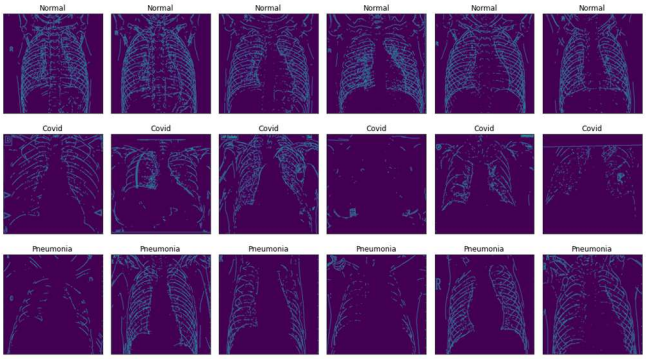

Fig. 11 Shows Canny edge detection that is performed on the x-ray images using the Canny() function imported from the cv2 library. We can observe that covid and pneumonia infected x-ray images have much less detail in them

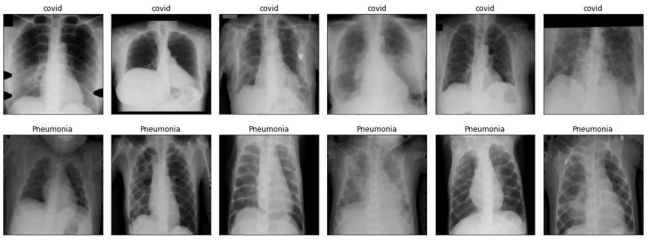

Fig. 12 Shows image erosion that is performed on the x-rays images using the erode() function imported from the cv2 library. Here too, we can observe that covid and pneumonia infected x-ray images are blurry than the normal ones.

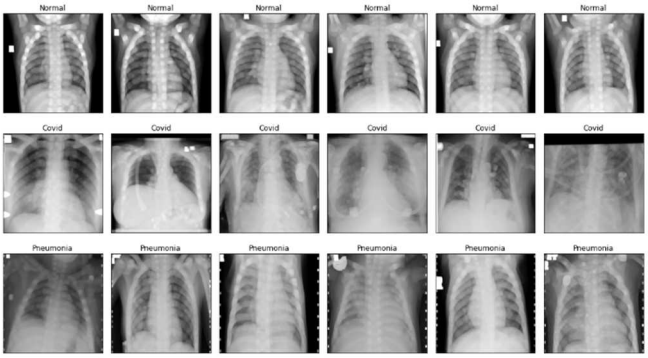

Fig. 13 Shows the chest x-ray images that are dilated using the dilate() function imported from the cv2 library. Here as well, we can observe a pattern that covid and pneumonia infected x-ray images are much blurrier than normal x-rays.

C. Data Preprocessing, Generation and Augmentation

Depending on the neural network employed, each picture is required to be preprocessed. Resizing and normalization have been performed on the images. According to their design, the neural networks employed require pictures of varying sizes. A 224x224 picture was required for ResNet50V2, MobileNetV2, and VGG16, whereas InceptionV3 calls for a 229x229 image. Various model designs were taken into account while normalizing the dataset.

D. Model creation and fine-tuning

In this study, Google Collaboratory, with runtime type set to GPU, was utilized to train, assess, visualize and test discrete CNN architectures. The dataset was subjected to pre-processing and then was trained using CNN architectures: VGG16, ResNet50V2, InceptionV3, and MobileNetV2, and then the performance of each of these architectures was tested on the test dataset. For each of the architectures, a base model was created by removing its top layer and keeping the rest of its layers frozen. In addition to the Global Average Pooling (GAP) layer, a Fully Connected layer of 128 neurons with activation set to ReLu was added to the basic model, followed by a dropout layer that had a keeping rate of 0.20. Last but not least, a logistic layer consisting of one neuron with softmax activation at the end, which may be used to forecast output class probabilities. Fig. 14 below depicts additional layers created over the base model.

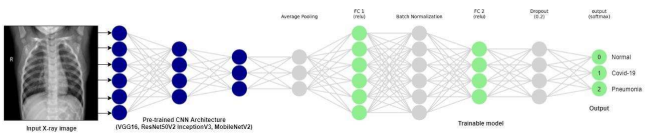

Fig. 14 Additional layers created over base the model architecture.

While training the models, the learning rate is lowered as the training progresses. This is done by applying the exponential decay function to the optimizer step, with an initial learning rate of 1e-3 and the decay rate set to 0.9. All the models have been initially trained for 15 epochs. The models have been then set to a learning rate of 1e-5 with the decay rate being 0.9. Early stopping has been introduced which stops the training process when the model performance starts becoming stagnant, or when the model starts overfitting to the training data.

VI. RESULT ANALYSIS

The performance of a classification model can be measured through a confusion matrix. It is represented in a matrix form. It gives the comparison between actual and predicted outputs. In a N x N matrix, the N is the number of classes or outputs. Thus, for 3 classes, we have a 3x3 matrix. Confusion Matrix is divided into true positive, false negative, false positive, and true negative. Commonly, classification models are evaluated by using particular metrics based on the values in a confusion matrix. The most popular classification metric is accuracy, which measures a classifier's overall performance.

Other common metrics are precision, recall (formally named sensibility), and the Fl-Score. Also handy is a graph showing the area under the curve (AUC). Precision is the fraction of correctly predicted true cases among the true cases predicted, whereas recall is the fraction of true cases that were retrieved from all the predictions. The weighted average of Precision and Recall will give the F1 score.

The dataset contains 6902 images separated into train, test, and val data each containing three classes normal, covid, and pneumonia. The test data contains 1379 images, the train data contains 4830 images while the remaining 693 images are used for validation.

At the beginning of training, the neural networks were using pre-trained ImageNet weights, later training and fine-tuning were performed as explained in the methodology in the above chapter. Accuracy, Area Under the Curve, precision, and recall are employed as metrics. These metrics were also used to monitor the performance on validation data after every epoch. Following are the graphs of each metric vs number of epochs for every model.

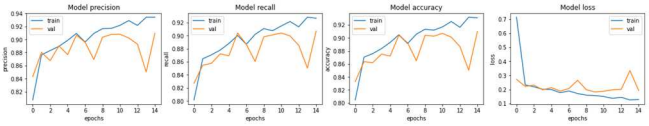

Fig.15 Graphical representation of different metrics of InceptionV3, before fine-tuning.

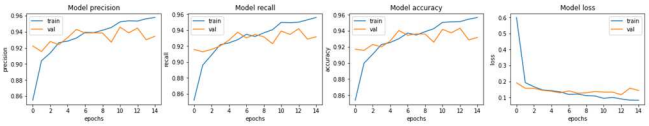

Fig.16 Graphical representation of different metrics of ResNet50V2, before fine-tuning.

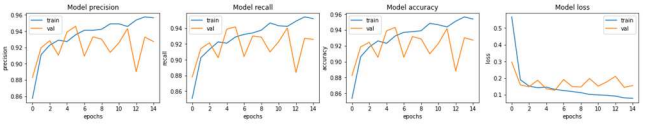

Fig.17 Graphical representation of different metrics of MobileNetV2, before fine-tuning.

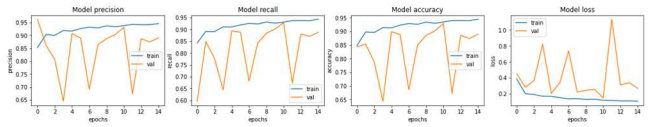

Fig.18 Graphical representation of different metrics of VGG16, before fine-tuning.

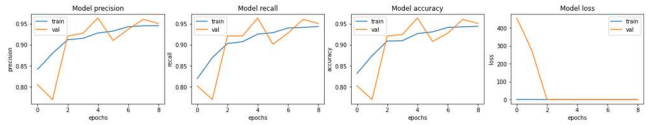

Fig.19 Graphical representation of different metrics of InceptionV3, after fine-tuning.

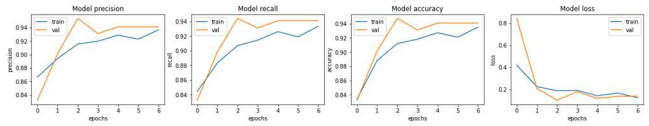

Fig.20 Graphical representation of different metrics of ResNet50V2, after fine-tuning.

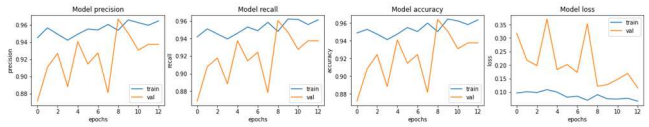

Fig.21 Graphical representation of different metrics of MobileNetV2, after fine-tuning.

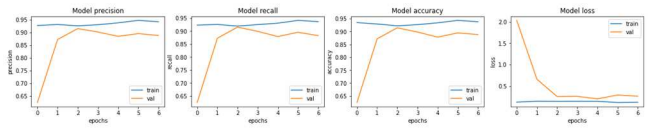

Fig.22 Graphical representation of different metrics of VGG16, after fine-tuning.

Among the four neural network architectures tested, the InceptionV3 model performed the best, followed by RestNet50, MobileNetV2, and VGG16 respectively. The detailed evaluation report is presented in Fig no.15-22 which shows confusion matrices for every neural network. Table no.1-2 shows the classification report containing accuracy, recall, f1-score, support for every model, and table no. 3-4 shows correct and wrong detection of each class by every model.

TABLE I. THE FOUR CNN'S TESTING ACCURACY, PRECISION, RECALL AND F1-SCORE; BEFORE FINE-TUNING

Model	Class	Precision	Recall	F1-score	Support
InceptionV3	Normal	0.90	0.92	0.91	453
	Covid	0.83	0.91	0.87	463
	Pneumonia	0.98	0.86	0.91	463
	Accuracy			0.90	1379
	Macro avg	0.90	0.90	0.90	1379
	Weighted avg	0.90	0.90	0.90	1379
ResNet50V2	Normal	0.96	0.97	0.96	453
	Covid	0.88	0.96	0.92	463
	Pneumonia	0.99	0.89	0.93	463
	Accuracy			0.94	1379
	Macro avg	0.94	0.94	0.94	1379
	Weighted avg	0.94	0.94	0.94	1379
MobileNetV2	Normal	0.94	0.97	0.96	453
	Covid	0.91	0.92	0.92	463
	Pneumonia	0.95	0.91	0.93	463
	Accuracy			0.93	1379
	Macro avg	0.93	0.93	0.93	1379
	Weighted avg	0.93	0.93	0.93	1379
VGG16	Normal	0.91	0.91	0.91	453
	Covid	0.92	0.80	0.86	463
	Pneumonia	0.82	0.93	0.88	463
	Accuracy			0.88	1379
	Macro avg	0.88	0.88	0.88	1379
	Weighted avg	0.88	0.88	0.88	1379

TABLE II. THE FOUR CNN'S TESTING ACCURACY, PRECISION, RECALL AND F1-SCORE; AFTER FINE-TUNING

Model	Class	Precision	Recall	F1-score	Support
InceptionV3	Normal	0.98	0.97	0.97	453
	Covid	0.90	0.98	0.94	463
	Pneumonia	1.00	0.92	0.95	463
	Accuracy			0.96	1379
	Macro avg	0.96	0.96	0.96	1379
	Weighted avg	0.96	0.96	0.96	1379
ResNet50V2	Normal	0.98	0.95	0.96	453
	Covid	0.89	0.97	0.93	463
	Pneumonia	0.98	0.92	0.95	463
	Accuracy			0.95	1379
	Macro avg	0.95	0.95	0.95	1379
	Weighted avg	0.95	0.95	0.95	1379
MobileNetV2	Normal	0.94	0.97	0.96	453
	Covid	0.90	0.93	0.91	463
	Pneumonia	0.96	0.91	0.94	463
	Accuracy			0.94	1379
	Macro avg	0.94	0.94	0.94	1379
	Weighted avg	0.94	0.94	0.94	1379
VGG16	Normal	0.97	0.81	0.88	453
	Covid	0.80	0.94	0.87	463
	Pneumonia	0.92	0.91	0.91	463
	Accuracy			0.89	1379
	Macro avg	0.90	0.89	0.89	1379
	Weighted avg	0.90	0.89	0.89	1379

TABLE III. CONFUSION MATRIX OF THE FOUR CNN MODELS; BEFORE FINE-TUNING

Model (epochs)	Normal			Covid			Pneumonia		
	Correct	*Falsely Detected*	*Not Detected*	*Correct*	*Falsely Detected*	*Not Detected*	*Correct*	*Falsely Detected*	*Not Detected*
InceptionV3(15)	417	48	36	423	86	40	396	9	67
ResNet50V2(15)	438	19	15	444	61	19	411	6	52
VGG16(15)	410	39	43	372	34	91	432	92	31
MobileNet (15)	440	27	13	428	43	35	420	21	43

TABLE IV. CONFUSION MATRIX OF THE FOUR CNN MODELS; AFTER FINE-TUNING

Model (epochs)	Normal			Covid			Pneumonia		
	Correct	*Falsely Detected*	*Not Detected*	*Correct*	*Falsely Detected*	*Not Detected*	*Correct*	*Falsely Detected*	*Not Detected*
InceptionV3(9)	438	9	15	456	51	7	424	1	39
ResNet50V2(7)	430	11	23	450	57	13	424	7	39
VGG16(7)	365	11	88	435	107	28	422	39	41
MobileNet(13)	439	26	14	429	46	34	423	16	40

VII. CONCLUSION

The proposed work implemented four CNN models (VGG16, ResNet50V2, InceptionV3, and MobileNetV2) for covid, pneumonia detection. As evident from the results, the InceptionV3 model performs best, providing an accuracy of 96%. Therefore, our results prove that the InceptionV3 model can be effectively used for the medical classification problem of covid and pneumonia detection. However, both ResNet50V2 and MobileNetV2 models closely follow the InceptionV3 model providing an accuracy of 95% and 94% respectively. As we know MobileNetV2 model provides good performance while using less computational resources, used esp. in embedded and mobile systems. Thus, the classification problem of detecting COVID-19 and Pneumonia can be performed using MobileNetV2. In the future when a substantially larger covid-19 dataset is available, these models can be trained again on this larger dataset with a much higher number of epochs while training. This might provide us with even better results. Additionally, these models can be further fine-tuned by changing hyperparameters such as batch size, activation function, learning rate, etc. A grid search can be tried for different mini-batch sizes (8, 16, 32, …).

VIII. ACKNOWLEDGMENT

Authors thank Dr. Vrushali Kulkarni HOS, School of Computer Engineering and Technology, MIT World Peace University, Pune, India, for providing all kinds of facilities and support.

IX. REFERENCES

[1] Johnson S., Wells D., Healthline Viral Pneumonia: Symptoms, Risk Factors, and More. [(accessed on 31 December 2019)]; Available online: https://www.healthline.com/health/viral-pneumonia.

[2] Pneumonia. [(accessed on 31 December 2019)]; Available online: https://www.radiologyinfo.org/en/info.cfm?pg=pneumonia.

[3] N. Liu, L. Wan, Y. Zhang, T. Zhou, H. Huo and T. Fang, "Exploiting Convolutional Neural Networks With Deeply Local Description for Remote Sensing Image Classification," in IEEE Access, vol. 6, pp. 11215-11228, 2018, doi: 10.1109/ACCESS.2018.2798799.

[4] Hosny A., Parmar C., Quackenbush J., Schwartz L.H., Aerts H.J. Artificial intelligence in radiology. *Nat. Rev. Cancer.* 2018;18:500–510. doi: 10.1038/s41568-018-0016-5.

[5] Kalchbrenner, N.; Grefenstette, E.; Blunsom, P. A convolutional neural network for modelling sentences. arXiv 2014, arXiv:1404.2188.

[6] Kim, Y. Convolutional neural networks for sentence classification. arXiv 2014, arXiv:1408.5882.

[7] Conneau, A.; Schwenk, H.; LeCun, Y.; Barrault, L. Very deep convolutional networks for text classification. arXiv 2016, arXiv:1606.01781.

[8] Huang G., Liu Z., Van Der Maaten L., Weinberger K.Q. *Proceedings of the IEEE Conference on Computer Vision and Pattern Recognition*. 2017. Densely connected convolutional networks; pp. 4700–4708.

[9] Krizhevsky A., Sutskever I., Hinton G.E. *Advances in Neural Information Processing Systems.* 2012. Imagenet classification with deep convolutional neural networks; pp. 1097–1105.

[10] M. I. Razzak, S. Naz, and A. Zaib, "Deep learning for medical image processing: overview, challenges and the future," *Lecture Notes in Computational Vision and Biomechanics*, vol. 32, pp. 323–350, 2018.

[11] Ü. H. Ayan, "Diagnosis of pneumonia from chest X-ray images using deep learning," in *Proceedings of the 2019 Scientific Meeting on Electrical-Electronics & Biomedical Engineering and Computer Science (EBBT)*, pp. 1–5, Istanbul, Turkey, April 2019.

[12] K. Simonyan, A. Zisserman, Very Deep Convolutional Networks for Large-Scale Image Recognition, arXiv preprint arXiv:1409.1556.

[13] Jain, R.; Nagrath, P.; Kataria, G.; Kaushik, V.S.; Hemanth, D.J. Pneumonia detection in chest X-ray images using convolutional neural networks and transfer learning. Measurment 2020, 165.

[14] Ayan, E., & Ünver, H. M. (2019, April). Diagnosis of Pneumonia from Chest X-Ray Images Using Deep Learning. In 2019 Scientific Meeting on Electrical-Electronics & Biomedical Engineering and Computer Science (EBBT) (pp. 1-5). IEEE

[15] Liang, G., & Zheng, L. (2019). A transfer learning method with deep residual network for pediatric pneumonia diagnosis. Computer methods and programs in biomedicine, 104964.

[16] [C1]Gaur, L., Bhatia, U., Jhanjhi, N.Z. et al. Medical image-based detection of COVID-19 using Deep Convolution Neural Networks. Multimedia Systems (2021). https://doi.org/10.1007/s00530-021-00794-6

[17] [C2]Zhenjia Yue, Liangping Ma, Runfeng Zhang, "Comparison and Validation of Deep Learning Models for the Diagnosis of Pneumonia", Computational Intelligence and Neuroscience, vol. 2020, Article ID 8876798, 8 pages, 2020. https://doi.org/10.1155/2020/8876798

[18] Cohen, J. P., Morrison, P., and Dao, L., "COVID-19 Image Data Collection", *arXiv e-prints*, 2020.https://github.com/agchung

[19] Winther, Hinrich B.; Laser, Hans; Gerbel, Svetlana; Maschke, Sabine K.; B. Hinrichs, Jan; Vogel-Claussen, Jens; et al. (2020): COVID-19 Image Repository. figshare. Dataset. https://doi.org/10.6084/m9.figshare.12275009.v1

[20] Kermany, Daniel; Zhang, Kang; Goldbaum, Michael (2018), "Labeled Optical Coherence Tomography (OCT) and Chest X-Ray Images for Classification", Mendeley Data, V2, doi: 10.17632/rscbjbr9sj.2

[21] NIH Chest X-rays, National Institutes of Health Chest X-Ray Dataset, Aug. 2017. [Online]. Available: https://www.kaggle.com/nih-chest-xrays/data